

# Plucked Piezoelectric Bimorphs for Knee-joint Energy Harvesting: Modelling and Experimental Validation

Michele Pozzi\* and Meiling Zhu

Department of Materials, School of Applied Sciences

Cranfield University, Bedfordshire, MK43 0AL, UK

\*e-mail: m.pozzi@cranfield.ac.uk (Corresponding author)

## Abstract

The modern drive towards mobility and wireless devices is motivating intense research in energy harvesting (EH) technologies. To reduce the battery burden on people, we propose the adoption of a frequency up-conversion strategy for a new piezoelectric wearable energy harvester. Frequency up-conversion increases efficiency because the piezoelectric devices are permitted to vibrate at resonance even if the input excitation occurs at much lower frequency. Mechanical plucking-based frequency up-conversion is obtained by deflecting the piezoelectric bimorph via a plectrum, then rapidly releasing it so that it can vibrate unhindered; during the following oscillatory cycles, part of the mechanical energy is converted into electrical energy. In order to guide the design of such harvester, we have modelled with finite element methods the response and power generation of a piezoelectric bimorph while it is plucked. The model permits the analysis of the effects of the speed of deflection as well as the prediction of the energy produced and its dependence on the electrical load. An experimental rig has been set up to observe the response of the bimorph in the harvester. A PZT-5H bimorph was used for the experiments. Measurements of tip velocity, voltage output and energy dissipated across a resistor are reported. Comparisons of the experimental results with the model predictions are very successful and prove the validity of the model.

**Keywords:** Plucked piezoelectric bimorphs, frequency up-conversion, energy harvesting, and human walking

## 1. Introduction

In recent years, low power consumption electronic devices have become pervasive. Electronic gadgets, including mobile phones, music players and navigation assistants, are at the centre of a very large consumer market; medical health monitoring devices improve the quality of life of many patients by offering them greater freedom of movement. Electronic miniaturization has brought about smaller and lighter devices that are more portable. However, it is generally felt, both within the electronic industry professionals and the consumers, that we are still enslaved by the need to constantly recharge batteries and therefore that the most desired feature in electronic devices is freedom from batteries.

The research community, within both academia and industry, has been addressing these problems for a decade now, with efforts focussed on the development of batteries with higher energy densities and on the development of alternative sources of energy, such as micro-generators [1] and energy harvesting (EH) [2]. Since the beginning, interest has been concentrated on the scavenging of energy from environmental vibrations, particularly for applications in wireless sensor networks, as many such sensors are not easily accessible for battery replacement [2]. More recently, more research efforts have been directed towards human-based EH, aiming at powering general consumer devices. An excellent example of energy harvesting from the mechanical dissipative work taking place during normal gait was presented in [3]. The authors developed an electromagnetic device capable of producing  $4.8 \pm 0.8$  W in the generative-braking mode during human walking. The only apparent limitations of the device are its mechanical complexity and the considerable mass of 790 g (1.6 kg including braces). Part of the mass and the mechanical complexity was due to the implementation of

gears which increase the rotational speed of the electromagnetic generator to increase its efficiency. In this paper, we study a device inspired by similar principles but based on piezoelectric bimorphs which are plucked while the wearer is simply walking.

Human activities, with the exception of vocalization, occur at very low frequencies, up to a few hertz. As is well known, piezoelectric bimorphs operating for sensing or energy generation are most effective at much higher frequencies. Devices of acceptable dimensions and mass for human integration and offering power outputs in the order of milliwatts have resonance frequencies of hundreds of hertz. This frequency mismatch between excitation and harvester makes it challenging to efficiently harvest energy from human motion with piezoelectric devices. The solution adopted in this paper is the implementation of mechanical means to effect an up-conversion of the frequencies, so that the piezoelectric bimorph vibrates at high frequency – in fact, at resonance – even if the external excitation occurs at a few hertz. This principle was initially presented by Umeda et al. [4] in the form of a piezoelectric monomorph disc impacted by a steel ball falling from a known height; as the ball bounced back off the disc, the latter vibrated at its resonance frequency, generating electrical energy. A hand-held prototype harvester based on this principle was realized by Renaud et al. [5]: as the harvester is rotated on a vertical plane or hand-shaken from side to side, a “missile” alternatively strikes one or the other of two piezoelectric elements placed at either end of the enclosure that contains it. Each bimorph is cyclically deformed as the missile strikes it and bounces off. Between impacts, the bimorph vibrates freely at resonance and generates energy (an output power up to  $600\mu\text{W}$  was produced with a vigorous “scratching” motion). A device based on a similar shock excitation but with dimensions in the order of millimetres was designed and prototyped by Cavallier et al. [6]. Rastegar et al. [7] introduced a different form of excitation for use on platforms which are slowly rocking side to side or vibrating at low frequencies. Whilst in Umeda's device energy is put in the piezoelectric transducer by impact (like wires are struck by hammers in a piano), in Rastegar's design the piezoelectric devices are more slowly deformed and then released (like chords are plucked in a harpsichord). Several concept designs for energy-harvesters based on a mechanical or magnetic up-conversion strategy were presented later by Rastegar and Murray [8]. In all designs, the fundamental principle is the transfer of energy from a “primary system”, directly coupled to a low frequency input, to a “secondary vibrating system” with higher resonant frequency. Sari et al. [9] have applied the principle of frequency up-conversion via plucking to the microscale and prototyped an electromagnetic generator where the low-frequency vibration of a suspended magnet excites the high frequency vibration of a number of coil-carrying cantilevers placed around it. The conversion of low frequency cyclic translations into higher frequency motion was implemented by Howells [10] with the Heel Strike Generator, where a system composed of lead screw, gear train and cam produced the controlled sinusoidal deformation of four PZT-5A elements. A fundamental difference between this technique and the one we are implementing is that Howell's bimorphs move at a frequency below resonance as they are always guided by the cam. An interesting piezoelectric harvester not based on seismic oscillation but rather on the direct deformation of cantilevers was presented in 2005 by Priya [11]. Here the piezoelectric bimorphs oscillate between stops which are mounted on a shaft set into motion by an air flow, as in a conventional windmill. The paper also reports some simple analytical modelling for the device where a static deflection of the beam is assumed (which is an acceptable approximation as the bimorphs are deformed at frequencies much lower than their fundamental).

In the present work, we propose the use of a plucking-based frequency up-conversion strategy for energy harvesting on humans, with special focus on converting the low-frequency rotation of the knee joint into high-frequency vibration of a number of piezoelectric bimorphs. We analyse the motion and power output of a piezoelectric cantilever when plucked by a mechanical plectrum touching its tip: the cantilever is deflected with constant speed up to a given displacement, after which it is expected to be released by the loss of contact with the plectrum (their contact area is progressively reduced as they bend). As the displacement constraint is removed, we observe the free

vibrations of the cantilever, occurring at its resonant frequency, while the electrical energy produced is dissipated by a resistor placed across the device. This two-step action (deflection and release) simulates rather closely the envisaged operation of the piezoelectric harvester we are currently designing for human-based energy harvesting. We also model the device as it is harmonically excited by a force on its tip; this set of analyses is meant to bridge between the standard harmonic seismic excitation and the plucking action of interest. It should be mentioned that most of the literature on piezoelectric energy harvesting is still devoted to *vibrational* energy scavenging. As a result, it is possible to find many models, both analytical [12] and based on finite elements [13], where the cantilevers, most typically with an added mass on the tip, are subject to seismic excitation, usually of harmonic character. Other forms of excitation are much more rarely considered [14]. To the best of the authors' knowledge, the input of mechanical energy into a PEHD by sporadic mechanical plucking has never been modelled before. Yet, such analyses are necessary to identify the many design parameters of a mechanical up-conversion harvester, such as piezoelectric material, frequency of plucking actions, dimensions of the piezoelectric bimorphs, number and spacing of the plectra that deflect the bimorphs and so on. The development of such an instrument is the main objective of this paper.

## 2. Frequency up-conversion by mechanical plucking

As discussed in the introduction, mechanical plucking is here proposed as a frequency up-conversion strategy in EH to bridge between the low-frequency inputs from human activities and the high-frequency requirements of piezoelectric devices. Mechanical plucking is constituted of a sequence of phases represented schematically in Figure 1. In the approach phase, the distance between bimorph and plectrum is reduced until contact is made. Immediately follows the loading phase, during which both elastic elements are deflected, according to their mechanical compliance. As the deflection progresses, the overlap between the two elements is reduced so that their contact area becomes gradually smaller. A limiting deflection is reached when the contact is lost and each element is free to return to its undeformed shape; this is the release point. From this instant on, the bimorph vibrates at its resonance frequency around its rest position as a cantilever beam. As the bimorph vibrates, the stored mechanical energy is converted by the direct piezoelectric effect into electrical energy and transferred to the external circuit; part of the mechanical energy is dissipated through various forms of damping, like air damping, dielectric losses and material internal damping. The outcome of plucking is frequency up-conversion, as by one single slow movement of the plectrum a large number of vibrations are produced at high frequency.

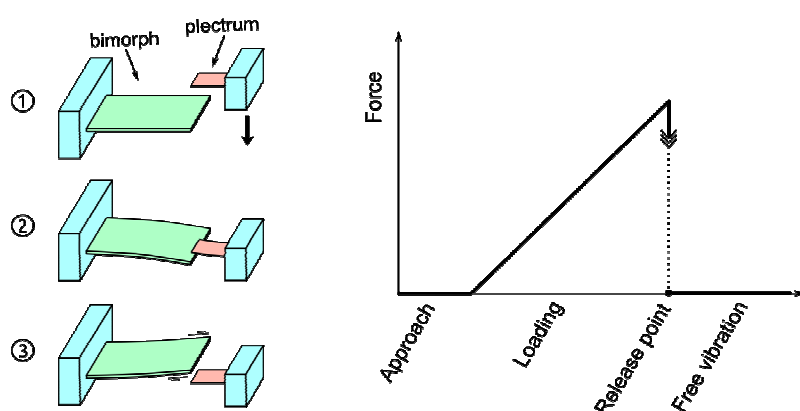


Figure 1. Illustration of the plucking action: 1) approach; 2) loading step with deflection of bimorph and plectrum; 3) release step followed by vibration of the bimorph at its resonance frequency. The plot shows the evolution of the external force applied at the tip of the bimorph as the plucking action progresses.

A knee-joint harvester that ensures the repetition of the plucking actions to achieve sustained power production is sketched in Figure 2. During normal gait, for example while walking, the knee alternatively bends and extends once per second, covering a rotation angle of approximately 70 degrees. With reference to the figure, the outer ring, carrying the plectra, is fixed to the thigh, whilst the internal hub, carrying the bimorphs, rotates with the knee as it is fixed to the shank. As the person walks and the knee alternatively extends and bends, each of the multiple plectra on the outer ring plucks the bimorphs according to the sequence outlined in Figure 1. The energy harvester is therefore capable of converting the slow motion of walking into high-frequency vibrations of several piezoelectric bimorphs. It is expected that the design has the potential to produce a sustained power of several milliwatts during walking.

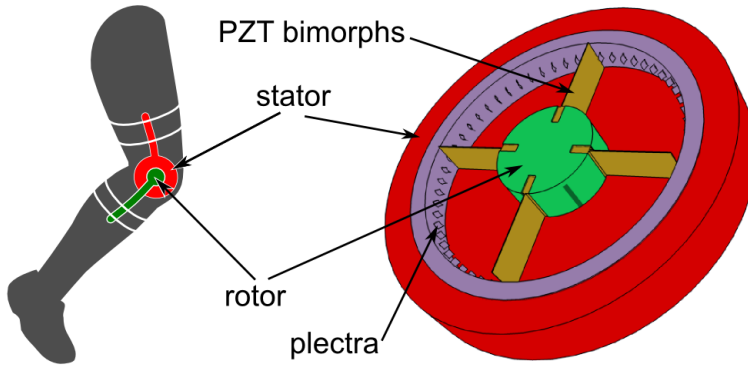


Figure 2: Knee joint piezoelectric harvester. It is worn on the external side of the knee and fixed by braces. Inside, a hub carries a number of bimorphs which are plucked by the ring-mounted plectra as the joint rotates during normal walking.

### 3. Modelling approach and experimental methods

#### 3.1. Finite Element Modelling

Finite Element (FE) modelling was performed using the commercial package ANSYS 11.0 (ANSYS Inc. Canonsburg, PA, USA). The analysis is based on SOLID5 piezoelectric elements, SOLID45 structural elements and uses CIRCU94 elements for the resistor placed across the electrodes of the bimorph. The power output is calculated from the voltage difference between the two electrodes, i.e. the voltage across the resistor. The boundary conditions include displacement constraints on the top and bottom surfaces in the clamped portion of the beam. The device modelled is a series bimorph with an internal brass shim and two sheets of PZT on either side, covering the entire surface (see details of geometrical measurements and material properties in Table 1). The choice of bimorph geometry was dictated by considerations of the acceptable dimensions of the overall harvester.

The model includes viscous damping with the damping matrix  $C$  given by:

$$C = \beta_{PZT} K_{PZT} + \beta_{brass} K_{brass}$$

where:

$\beta_{PZT}$  and  $\beta_{brass}$  = stiffness matrix multiplier for PZT and brass

$K_{PZT}$  and  $K_{brass}$  = portion of structure stiffness matrix based on PZT and brass

The  $\beta$  parameter was calculated from the tabulated mechanical quality factor  $Q_m$  and the resonant frequency of the device as

$$\beta = \frac{1}{\omega Q_m}$$

according to section 5.9.3 of the ANSYS 11 *Structural Analysis Guide*. Two types of analyses were performed: harmonic and transient. During the harmonic analysis, a sinusoidally varying force of 10 mN was applied at the tip and its frequency was scanned in the neighbourhood of the first resonant frequency of the structure. This analysis is similar to the conventional analyses in [13], where the cantilever, with a large mass applied on its tip, is seismically excited by the vibration of its base. In the present case, the force, rather than being of “inertial” origin and distributed along the cantilever, is localized on the nodes at the tip. The power output during the harmonic analysis was calculated as root-mean-square power using the amplitude voltage  $V_0$  detected across the resistor R:

$$P_{rms} = \frac{V_0^2}{2R}$$

Table 1. Geometrical parameters of the model and materials properties.

<b>Geometry</b>	
Total length	30 mm
Free length	25 mm
Width	10 mm
Total thickness	400 $\mu\text{m}$
PZT thickness	150 $\mu\text{m}$
<b>Material properties (PZT-5H)</b>	
Density	7800 kg/m <sup>3</sup>
$c_{11}^E$	62 GPa
$c_{33}^E$	50 GPa
$d_{31}$	-320 $10^{-12}$ m/V
$d_{33}$	650 $10^{-12}$ m/V
$\epsilon_{11}^T$	3600
$\epsilon_{33}^T$	3800
$Q_m$	32
<b>Material properties (brass)</b>	
Elasticity modulus	100 GPa
Density	8700 kg/m <sup>3</sup>
$Q_m$	$2.5 \cdot 10^3$

The transient analysis was divided into two steps to clarify the effects of different conditions applied during each step without the interference of the other one. The first is a loading step, during which the bimorph was deflected at constant speed to a predefined tip displacement. In the FE model, this was achieved with a ramped load solution step where the nodes at the tip were constrained to the desired deflection (only displacements in the direction of approach were so constrained, to permit bending without stretching). This approximates the effect of a plectrum which comes into contact with the bimorph and, moving at constant speed, deflects it, as seen in Figure 1. The following step is the release phase and was modelled in a second transient analysis, starting with a stepped removal of the tip constraints of a statically deflected beam. The solution was obtained at a large number of sub-steps so as to adequately resolve the response of the device for several milliseconds until the

amplitude of vibration was quite small.

In transient analyses, the instantaneous power  $P(t_i)$  at substep  $i$  was calculated from the voltage across the resistor at the same substep:

$$P(t_i) = \frac{V^2(t_i)}{R} \quad 1$$

From this, the average power  $P_{av}$  produced up to the time  $t_n$  can be calculated according to the following expression:

$$P_{av}(t_n) = \frac{1}{t_n} \sum_{i=0}^n P(t_i) \Delta t_i \quad (\text{for } n > 0) \quad 2$$

where  $\Delta t_i$  is the duration of each substep. The average power is of particular interest in the release phase, as it permits to optimize the interval between plucking actions and to predict the ensuing sustained power.

Finally, the instantaneous power is also used to calculate the cumulative energy produced up to substep  $n$  :

$$E(t_n) = \sum_{i=0}^n P(t_i) \Delta t_i \quad 3$$

Naturally,  $E(t_n)$  will be a monotonic function of time.

### 3.2. Experimental details

Harmonic response measurements with seismic excitation were performed with the experimental equipment and methods already described in [15], with the notable difference of the addition of a Laser Doppler Vibrometer (Polytec CLV-2534) which was used to measure the velocity of vibrations. The closest match to the bimorph specified in Table 1 available commercially was found in the piezoelectric bimorphs type T215-H4-303X produced by Piezo Systems Co.; their dimensions are  $31.8 \times 12.7 \times 0.38 \text{ mm}^3$ , they are made of PZT-5H and they are poled for series operation. A  $130 \text{ }\mu\text{m}$ -thick metal shim is sandwiched between two layers of PZT, each of thickness  $125 \text{ }\mu\text{m}$ . For the harmonic response test, a sample was mounted within copper-clad mechanical fixtures doubling up as pick-off electrodes, leaving a free length of about  $22.5 \text{ mm}$ . Seismic excitation took place with an acceleration of approximately  $7.1 \text{ m/s}^2$ .

The plucking excitation, illustrated in Figure 1, was produced by loading the bimorph against a plectrum by displacing it over a given distance; release occurred upon retraction of the plectrum, mounted on a linear translation stage (Figure 3). Velocity data were collected with the Polytec LDV. A custom made fixture permits the mounting of the bimorph under test within copper-clad plates leaving a free length of  $26 \text{ mm}$ . The plectrum was a  $3 \times 2 \text{ mm}^2$  ( $l \times w$ ) rectangle cut out of a  $125 \text{ }\mu\text{m}$ -thick Kapton® polyimide film.

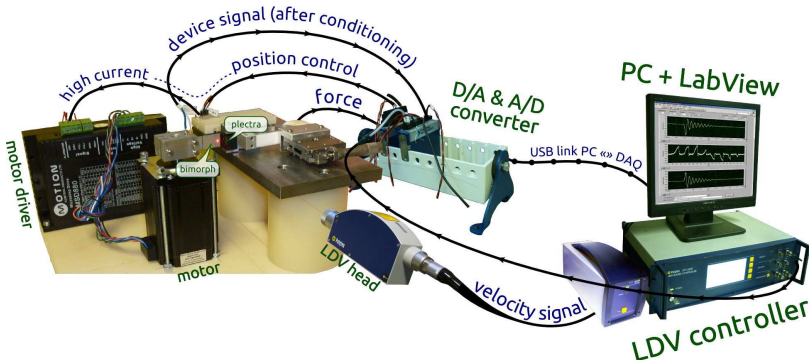


Figure 3. Layout and major connections of the experimental set-up used for plucking excitation. The conditioning circuit between bimorph and A/D converter, offering switchable electrical loads, is not shown.

Both in harmonic and plucking excitation tests, the output of the bimorph was connected to the same circuit described in [15], which supports electrical loads in multiples of 25 kΩ up to 550 kΩ; the output from the circuit was sampled and transferred to a computer.

## 4. Results and discussion

### 4.1. Simulated harmonic analyses

The harmonic analysis simulates the normal operating conditions of an environmental energy harvester. The power output curves for the piezoelectric bimorph with the parameters specified in Table 1 are reproduced in Figure 4 and correspond to maximum voltage amplitudes ranging from 2.7 mV at 300 Hz with 2 Ω up to 24 V at 320 Hz with 1 MΩ electrical load. The largest power output is found with an electrical load of 10 kΩ. As the electrical load increases, we observe a shift in the resonance frequency towards higher values; as is well known, this is due to the stiffening effect produced by the direct piezoelectric effect when the voltage on the electrodes is permitted to build up, which does not happen with lower resistors. The curve corresponding to 20 kΩ is particularly interesting as it has a maximum at frequencies intermediate between open and closed circuit and shows the largest area under the curve (it is lower but broader), indicating that it corresponds to maximum electrical damping, i.e. most efficient power transfer from the piezoelectric bimorph to the resistor, where it is dissipated. With 20 kΩ, a peak voltage amplitude of 6.1 V was detected at about 310 Hz.

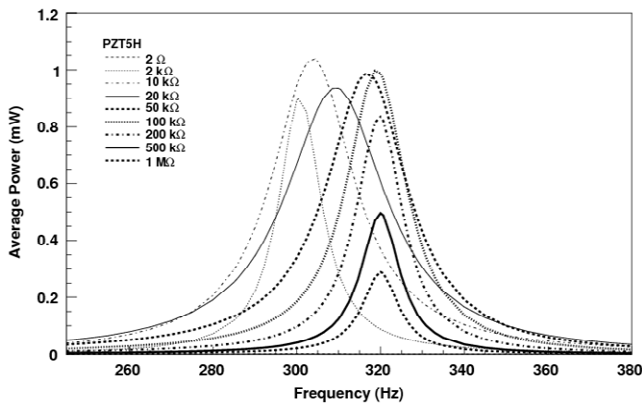


Figure 4. Predicted average electrical power output  $P = (V_0)^2/(2 \cdot R)$  from a PZT-5H bimorph under harmonic excitation; different curves correspond to different electrical loads (the curve for 2 Ω is almost undistinguishable from the x axis).

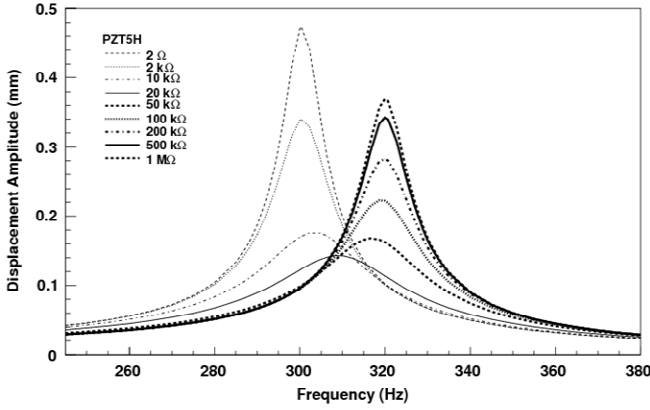


Figure 5. Predicted displacement amplitude of the tip of a bimorph made of PZT-5H under harmonic excitation and various electrical loads.

The picture is not complete without considering the corresponding displacements, which are plotted in Figure 5. The peak amplitude is minimum for the same resistor identified above as that corresponding to maximum electrical damping (20 kΩ).

A combined observation of Figure 4 and Figure 5 highlights the fact that the electrical loads for which higher power is produced are also associated with larger displacements. However, it is well known that excessive (tensile) strain in the piezoelectric ceramic can lead to a reduced operation life or even instantaneous failure, if particularly intense. It is therefore important to determine the resistor value that yields the maximum power whilst limiting the strain of the material. For this, it is necessary to define an appropriate figure of merit in order to identify the optimal electrical load. This parameter must factor out the displacement ( $\delta$ ) but at the same time include the effect of the electrical load. The quantity  $V/\delta$  is not suitable as the voltage increases monotonically with the load and we would not be able to identify the optimal load and the corresponding power produced. On the other hand,  $P/\delta$  is also not appropriate as the power depends on the square of the displacement (via the voltage). It is therefore here proposed the use of the quantity:

$$f(R) = \frac{\sqrt{P}}{\delta} \quad 4$$

In Figure 6 we have plotted the figure of merit defined in Equation 4 for the device considered: the best performance is obtained at 20 kΩ, where  $f = 6.8 \sqrt{mW} / mm$  at 311 Hz. This result confirms the qualitative impressions already gathered by looking at Figure 4 and Figure 5, where we commented that the wider curve found with the 20 kΩ resistor was indicative of large electrical damping, associated to efficient energy conversion.

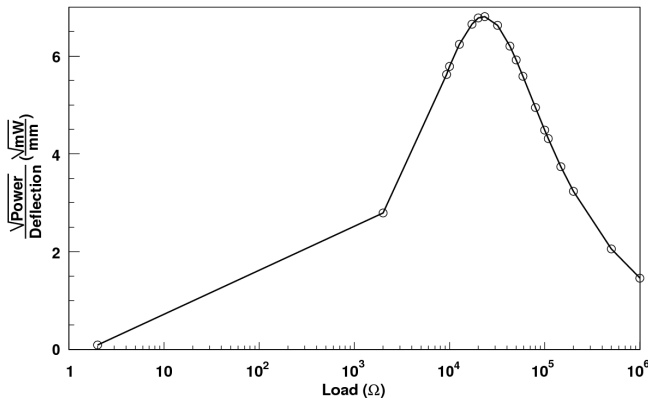


Figure 6. Calculated “figure of merit” as defined in Equation 4 to identify the optimal electrical load



of the PZT-5H bimorph under harmonic excitation.

## 4.2. Experimental harmonic response

The resonance frequency, tip displacement and voltage at resonance extracted from the experimental frequency response curves are tabulated in Table 2, which also reports the corresponding results from the model. The parameters fed to the FE model of the previous sections were modified to match the geometrical characteristics of the bimorph available for testing and the testing conditions. In particular, the free length was set at 22.5 mm, the quality factor was  $Q_m = 35$  (see section 4.5 for more details) and seismic excitation was applied, with the base subject to an acceleration of amplitude  $7.1 \text{ m/s}^2$ . From the table, it is seen that the resonance frequencies are predicted with an error typically less than 1 % with the only exception of the short circuit condition, where the mismatch is 2 %. The displacement is accurate within 2 %, again with the exception of the short circuit condition, where it is about 8%. It should be noted that the resistance of electrodes and contacts makes it impossible to realize an ideal short circuit condition in experiments. Finally, the voltage is generally underestimated by the model by 5 to 10 %. Overall, there is good agreement between experimental and modelling results.

Table 2. Peak location (on the frequency axis) and corresponding amplitudes of the frequency response curve: comparison between experiments and FEA for a selection of load resistors

Resistor	Experiment			FEA		
	Frequency (Hz)	Displacem. ( $\mu\text{m}$ )	Voltage (V)	Frequency (Hz)	Displacem. ( $\mu\text{m}$ )	Voltage (V)
S/C	363	67.1*	N/A	356	73.1	N/A
25 k $\Omega$	378	24.7	1.5	376	24.5	1.5
50 k $\Omega$	381	34.0	2.3	379	33.7	2.2
100 k $\Omega$	381	46.2	3.3	380	45.3	3.0
200 k $\Omega$	380	55.8	4.0	380	55.3	3.7
O/C	382	70.2	N/A	380	71.2	4.8

Note: \* The mismatch between experiment and model is partly due to the impossibility of realizing an ideal short-circuit condition in practice.

## 4.3. Simulated transient analysis: loading step

The transient analyses for the loading step were conducted with different deflection speeds to shed light on their effect on the power output. In real operation, specifically in a knee-joint harvester, the relative speed between plectrum and bimorph depend on the operating conditions, namely the phase of the gait cycle as the angular velocity of the knee joint is obviously not constant; the range of occurring speeds is also determined by the device geometry, in particular the radius of the plectra-carrying ring, so it is a factor that needs to be considered during design.

The plots in Figure 7 were obtained by modelling a PZT-5H bimorph connected to a resistive load of 20 k $\Omega$ . The choice of load is dictated by the fact that this value was found to yield the highest power in the following release step. As the energy produced is significantly larger in the release step than in the loading step, and it is not feasible to change the electrical load between the two steps in a real

harvester, precedence is given to the step with higher energy yield. The final imposed displacement is equal to 0.5 mm in all curves but the total time to reach full deflection is 2 ms in (a) and 5 ms in (b).

The ripples visible in the graphs are due to natural vibrational modes, as the input is a forced displacement of the tip with constant loading speed (ramped loads). Note that a ramp is the best approximation of the deformation that is likely to be experienced by the bimorph in a harvester using plucking as the frequency up-conversion strategy. What emerges from a first look at the graphs is that, having fixed the load resistor, both power and energy produced decrease as the deflection speed decreases. This is not surprising. If we assume that the total charge  $Q$  produced by deflecting the piezoelectric material depends only on the final strain, so in particular we disregard the higher modes of vibration, we have:

$$I = \frac{Q}{\Delta t} \text{ and so: } P = RI^2 = \frac{RQ^2}{\Delta t^2} \text{ or also: } E = \frac{RQ^2}{\Delta t} \quad 5$$

This relation between the energy  $E$  and the deflection time  $\Delta t$ , was asymptotically observed by the modelling results for slow deflections, as the higher modes become less important. This can be verified in Figure 8, which summarizes the effect of the speed of deflection on the energy produced.

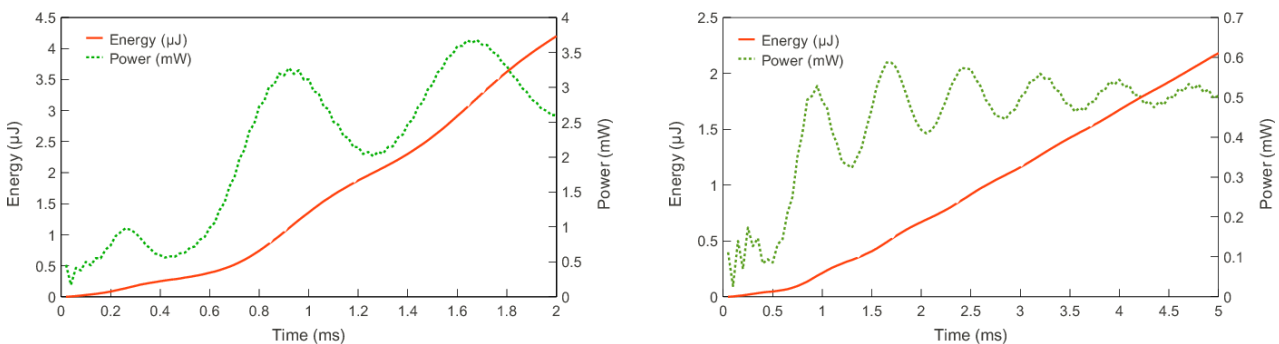


Figure 7. Predicted energy (solid red lines) and power (dashed green lines) outputs plotted versus time for a 0.5 mm deflection occurring in 2 ms and 5 ms, as indicated on the abscissa. The electrical load is 20 k $\Omega$  in both cases.

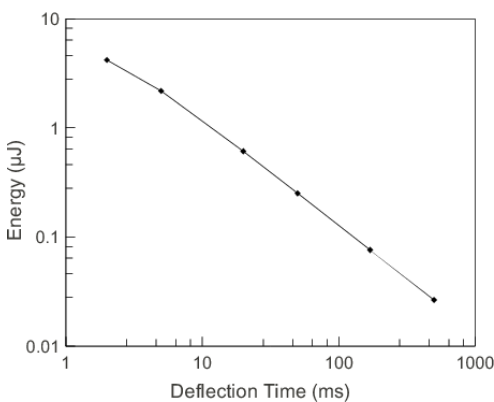


Figure 8. Predicted effect of the speed of deflection on the total energy produced in the loading step. The curve asymptotically approaches a straight line as the deflection time increases, in agreement with Equation 5

#### 4.4. Simulated transient analysis: release step

Perhaps the most interesting outcome of the FE analyses, and certainly the most useful results in view of the intended application, pertain to the behaviour of the cantilever upon release. With a full transient analysis, we analysed the vibrations of the piezoelectric device and looked at the power output at every substep, according to Equation 1.

Figure 9 and Figure 10 contain the plots of the cumulative energy (calculated according to Equation 3) and voltage, respectively, as a function of time. After being deflected very slowly by 0.5 mm, the cantilever is released at time 1 s and its dynamics is followed for several milliseconds. The deflection was set to occur over 1 s to ensure that velocities are zero at the time of release (the time axis starts at 1 s in the graphs as a reminder of this). The many curves in Figure 9 (cumulative energy) refer to different loading conditions, from 1  $\Omega$  to 500 k $\Omega$ , as specified on the plot. The voltage measured across a subset of resistors is plotted in Figure 10. An interesting feature apparent in the voltage across the 500 k $\Omega$  resistor is the fact that, despite oscillating, the voltage tends to stay negative and slowly drifts upwards. This is explained considering that the bimorph was quasi-statically deflected before release, while current flew through the external circuit. Therefore, just before release the bimorph is mechanically deflected but has free charges on the electrodes that balance the polarization-induced charges. To understand the behaviour upon release it is best to refer to an ideal open circuit situation; in this case, the voltage would remain negative, oscillating around a mid value until mechanical dissipation would bring the bimorph at rest, whilst the voltage would be determined by the free charge present at the beginning (which could not migrate due to the open circuit condition). This remnant voltage would also keep the bimorph somewhat deflected in the original direction. With finite resistors, the charges can migrate more or less quickly and eventually the bimorph reaches a static undeformed shape with equi-potential electrodes.

From the graphs, it is apparent that the bimorph produces 59  $\mu\text{J}$  across 20 k $\Omega$ . Table 3 collects the overall efficiency under different loads. In reading this table one must remember that the only damping taken into account is the internal damping of the material, while air damping and electrical or dielectric losses were neglected.

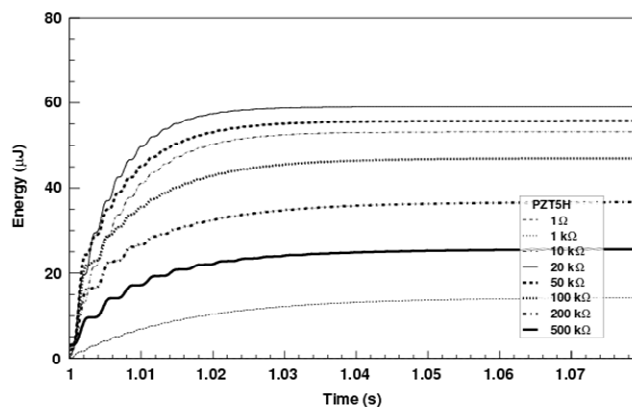


Figure 9. Predicted cumulative energy produced by the bimorph upon release after a deformation of 0.5 mm lasting 1 s. The slow deformation ensures that the bimorph is not vibrating at the time of release.

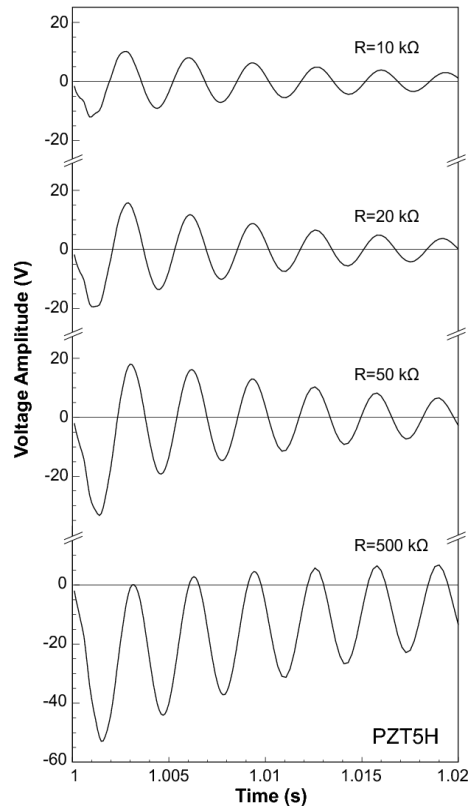


Figure 10. Predicted voltage amplitude produced by the bimorph upon release after a deformation of 0.5 mm lasting 1 s. The slow deformation ensures that the bimorph is not vibrating at the time of release. Only a subset of electrical loads is shown for conciseness.

Table 3. Energy conversion efficiency of the bimorph as ratio between electrical energy output and mechanical work done on the device during the loading step.

Resistance	Energy Conversion Efficiency
1 $\Omega$	~0%
1 k $\Omega$	16%
10 k $\Omega$	61%
20 k $\Omega$	<b>68%</b>
50 k $\Omega$	64%
100 k $\Omega$	54%
200 k $\Omega$	42%
500 k $\Omega$	30%

Although the largest energy is obviously produced from each stroke after an “infinite” time, the best strategy to maximize the overall power production of a practical harvester is to repeatedly pluck the bimorph, even before it has exhausted the mechanical energy put into it, i.e. while it is still vibrating. The plots in Figure 11 will be useful to anyone designing a PEHD based on the plucking principle. They represent the average power  $P_{av}$  produced up to the time  $t_n$  indicated on the  $x$ -axis, according to Equation 2. These graphs are to be used while deciding the optimal frequency of plucking actions. The average power increases rather rapidly in the first few milliseconds, and then it starts decaying – the first few oscillations are quite ample, but the amplitude decreases roughly exponentially and so does the additional energy produced; as Figure 9 shows, the total energy saturates rather quickly. The

highest power output is obtained when the plots in Figure 11 reach their maximum. However, at those times the bimorph is still vibrating with large amplitudes/speeds and a subsequent contact with the plectrum may occur at high speed, damaging the device. The plots of  $P_{av}$  show that if plucking actions occur every 5 to 10 ms, average powers in the range 5 to 7 mW can be achieved. As human activities are not perfectly repeatable, any human-integrated device is likely to operate over a wide range of conditions; this means that it is not possible to design a harvester working constantly at the optimal plucking frequency.

In addition, the electrical load that gives the maximum Figure of Merit (in Figure 6) is the one that gives the maximum average power (in Figure 11) in the time interval at which we intend to repeat the plucking. For the purpose of designing real devices, it is therefore appropriate to acquire frequency response curves for the device with different resistors and identify the one that maximizes the Figure of Merit defined in Equation 4. This will then represent the input resistance of the power management circuit that maximizes power transfer during plucking-based frequency up-conversion.

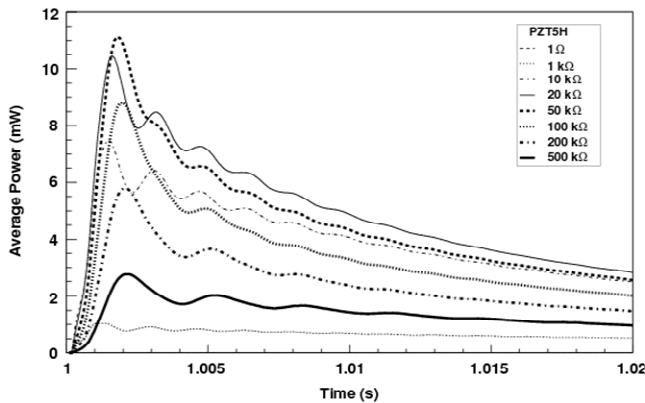


Figure 11. Predicted average power produced under different electrical loads in the first 20 ms upon release.

#### 4.5. Experimental plucking actions

In order to validate the model's predictions with respect to plucking excitation, experimental data were collected on a bimorph plucked by a plectrum while its terminals were connected to a 25 k $\Omega$  load. The velocity near the free end of the bimorph, the voltage output and the resulting energy are plotted in Figure 12 with solid lines; the figure also shows the results from the model (dashed lines). The geometrical input parameters of the model were modified to reflect the available bimorph and the testing conditions (in particular, the length of clamped region). As regards the initial conditions, since the initial deflection of the bimorph could not be directly measured with sufficient accuracy, the velocity – measured by LDV – was used instead. Specifically, the initial displacement of the tip of the bimorph was set in the model so that the first peak of the FE velocity data coincides with the first peak of the experimental data (this point is marked by a symbol on Figure 12). It was found that the initial condition that satisfies this requirement is a tip deflection of 88  $\mu\text{m}$ . The mechanical quality factor  $Q_m$  introduced in the FE model was calculated from the exponential decay of the vibrations recorded after a plucking excitation in open circuit conditions. The calculated value ( $Q_m=35$ ) differed slightly from that tabulated on the supplier's datasheet for the material ( $Q_m=32$ ).

It can be seen from Figure 12 that the model predictions are very accurate. The only disagreement between model and experiment occurs in the neighbourhood of the release time ( $t=0$  s). Whilst the model naturally predicts a prompt increase of velocity as soon as the displacement constraint is removed, the experimental data show an unclear start, with the velocity increasing more slowly and

also with some “noise” (just before  $t=0$  s). This can be explained by considering that both bimorph and plectrum have a thickness larger than the initial deflection and that their contact edges are not perfectly parallel. Therefore, when the overlap between plectrum and bimorph reduces, they rub against each other, causing some energy loss at the beginning and a “dirty” release. In fact, time-integration of the experimental velocity would suggest that initially (at  $t = -1$  ms in Figure 12), the bimorph is actually deflected by about  $120\ \mu\text{m}$ . This means that for the first  $32\ \mu\text{m}$  the bimorph is starting to spring back but is not completely free as contact with the plectrum persists. This is important for the harvesting device as it means that the full deflection of the bimorph, as defined by compatibility with the maximum deflection permitted, cannot be completely exploited at the moment. There is however scope for increasing the energy output by achieving a cleaner, sharper release. These tests show an energy generation exceeding  $2\ \mu\text{J}$ ; other tests, with larger deflections of the bimorph have produced approximately  $40\ \mu\text{J}$ .

As regards the frequency of oscillations, the agreement between model and experiment is very good with  $294\ \text{Hz}$  (model) vs.  $291\ \text{Hz}$  (experiment).

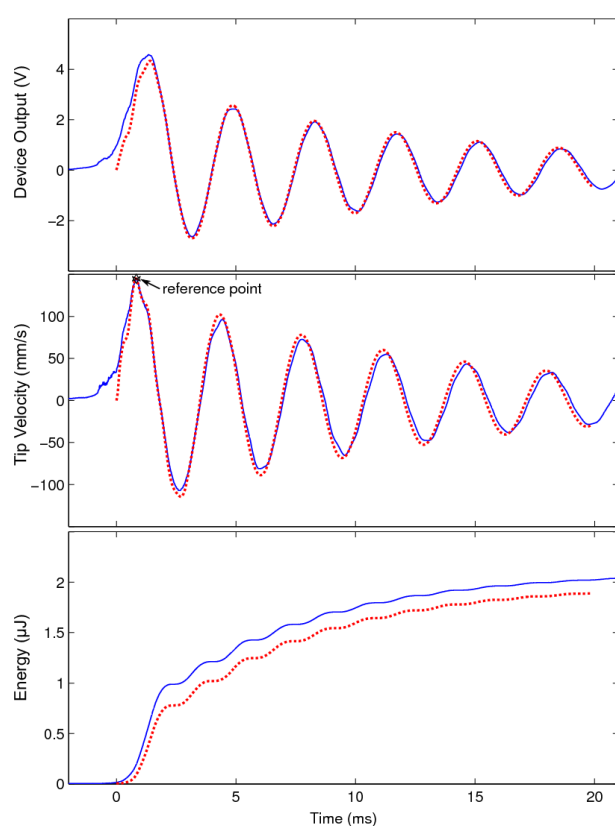


*Figure 12. Comparison between experimental results (solid blue line) and model (dashed red line) for plucking excitation. In the plots: voltage measured across a  $25\ \text{k}\Omega$  resistor, velocity of the tip and electrical energy dissipated by the resistor during a single plucking action. The symbol on the velocity plot indicates the point at which the model output velocity was matched to the experimental measurement.*

## 5. Conclusions

Piezoelectric energy harvesters often have to battle with contrasting frequency requirements: the available vibrations are low-frequency, but the harvester's active element performs best at high frequencies. For this reason, we propose to use mechanical plucking as the frequency up-conversion strategy for human-based EH. Bimorph plucking means that a piezoelectric bimorph is deflected by mechanical contact with a plectrum so that, when rapidly released, it may vibrate around its rest

position at its own resonant frequency. During these vibrations, an important portion of the elastic energy stored is converted into electrical energy.

In this paper we have presented a finite element model to simulate the response of a plucked bimorph, predicting voltage and energy dissipated across a resistor placed in series to the device. Although frequency up-conversion strategies have previous reports in the literature, as outlined in the introduction, it is the first time that the plucking mode of operation is systematically studied and modelled, with a view to human based energy harvesting. The results of this model give needed insight for the design of energy-harvesters based on plucking as the frequency up-conversion strategy. The model suggests that the optimal input resistance of the power management circuit can be estimated by running simple (and already very commonly employed) tests with harmonic seismic excitation.

We have reported experimental measurements, which fully validate the model. The model is very good at predicting both the frequency response of the bimorph in harmonic excitation and the transient response following a plucking action. A slight mismatch between model and experiment velocity data at the time of release has allowed us to identify the action of releasing the bimorph as a potentially major source of energy dissipation. More specifically, if the release is not sufficiently clean, as happens when the contact between plectrum and bimorph is lost over a significant distance of relative motion, the initial deflection of the bimorph cannot be fully exploited for energy generation.

We are currently working towards a human-based harvester exploiting the plucking strategy; the device will be worn on the knee and is expected to produce usable power sufficient to keep electronic gadgets, such as MP3 players or even mobile phones, permanently charged.

## **Acknowledgements**

This research is sponsored by the Engineering and Physical Sciences Research Council (EPSRC) via grant No. EP/H020764/1.

## **References**

- 1 S. Chou, W. Yang, K. Chua, J. Li, and K. Zhang, "Development of micro power generators - A review," *Applied Energy*, vol. In Press, Corrected Proof.
- 2 S.P. Beeby, M.J. Tudor, and N.M. White, "Energy harvesting vibration sources for microsystems applications," *Measurement Science and Technology*, vol. 17, 2006, pp. R175-R195.
- 3 J.M. Donelan, Q. Li, V. Naing, J.A. Hoffer, D.J. Weber, and A.D. Kuo, "Biomechanical Energy Harvesting: Generating Electricity During Walking with Minimal User Effort," *Science*, vol. 319, Feb. 2008, pp. 807-810.
- 4 M. Umeda, K. Nakamura, and S. Ueha, "Analysis of the Transformation of Mechanical Impact Energy to Electric Energy Using Piezoelectric Vibrator," *Japanese Journal of Applied Physics*, vol. 35, no. 1, pp. 3267-3273, 1996.
- 5 M. Renaud, P. Fiorini, R. van Schaijk, and C. van Hoof, "Harvesting energy from the motion of human limbs: the design and analysis of an impact-based piezoelectric generator," *Smart Materials and Structures*, vol. 18, no. 3, p. 035001, 2009.
- 6 B. Cavallier, P. Berthelot, H. Nouira, E. Foltete, L. Hirsinger, and S. Ballandras, "Energy harvesting using vibrating structures excited by shock," in *Ultrasonics Symposium, 2005 IEEE*, vol. 2, pp. 943-945, 2005.
- 7 J. Rastegar, C. Pereira, and H. Nguyen, "Piezoelectric-based power sources for harvesting energy

from platforms with low-frequency vibration,” *Smart Structures and Materials 2006: Industrial and Commercial Applications of Smart Structures Technologies*, E.V. White, Ed., San Diego, CA, USA: SPIE, 2006, pp. 617101-7

- 8 J. Rastegar and R. Murray, “Novel two-stage piezoelectric-based electrical energy generators for low and variable speed rotary machinery,” in *Proceedings of SPIE*, pp. 72880B-72880B-8, 2009.
- 9 I. Sari, T. Balkan, and H. Kulah, “An Electromagnetic Micro Power Generator for Low-Frequency Environmental Vibrations Based on the Frequency Upconversion Technique,” *Microelectromechanical Systems, Journal of*, vol. 19, 2010, pp. 14-27.
- 10 C.A. Howells, “Piezoelectric energy harvesting,” *Energy Conversion and Management*, vol. 50, Jul. 2009, pp. 1847-1850.
- 11 S. Priya, “Modeling of electric energy harvesting using piezoelectric windmill,” *Applied Physics Letters*, vol. 87, 2005, p. 184101.
- 12 A. Erturk and D.J. Inman, “A Distributed Parameter Electromechanical Model for Cantilevered Piezoelectric Energy Harvesters,” *Journal of Vibration and Acoustics*, vol. 130, 2008, pp. 041002-15.
- 13 M. Zhu, E. Worthington, and J. Njuguna, “Analyses of power output of piezoelectric energy-harvesting devices directly connected to a load resistor using a coupled piezoelectric-circuit finite element method,” *Ultrasonics, Ferroelectrics and Frequency Control, IEEE Transactions on*, vol. 56, no. 7, pp. 1309-1317, 2009.
- 14 A. M. Wickenheiser and E. Garcia, “Broadband vibration-based energy harvesting improvement through frequency up-conversion by magnetic excitation,” *Smart Materials and Structures*, vol. 19, no. 6, p. 065020, 2010.
- 15 M. Zhu and E. Worthington, “Design and testing of piezoelectric energy harvesting devices for generation of higher electric power for wireless sensor networks,” in *Sensors, 2009 IEEE*, pp. 699-702, 2009.